Waves in Random Media **8** (1998) 437–450. Printed in the UK PII: S0959-7174(98)93612-6

Inverse bounds for microstructural parameters of composite media derived from complex permittivity measurements

Elena Cherkaeva and Kenneth M Golden

Department of Mathematics, The University of Utah, Salt Lake City, UT 84112, USA

Received 23 April 1998

Abstract. Bounds on the volume fraction of the constituents in a two-component mixture are derived from measurements of the effective complex permittivity of the mixture, using the analyticity of the effective property. First-order inverse bounds for general anisotropic materials, as well as second-order bounds for isotropic mixtures, are obtained. By exploiting an analytic representation of the effective complex permittivity, the problem of estimating the structural parameters is reduced to a problem of evaluating the moments and support of a measure containing information about the geometrical structure of the material. Rigorous bounds on the volume fraction are found by inverting first- and second-order (Hashin–Shtrikman) forward bounds on the complex permittivity. The inverse bounds are applied to measurements of the effective complex permittivity of sea ice, which is a three-component mixture of ice, brine and air. The sea ice is treated via the two-component theory applied to a mixture of brine and an ice/air composite. The bounds on the brine volume of sea ice derived from the effective permittivity measurements are in excellent agreement with data from experiments. The inversion of forward bounds on the complex permittivity of composite media provides a basis for a theory of inverse homogenization for recovering microstructural parameters from bulk property measurements. Such results are applicable to problems in remote sensing, medical imaging and non-destructive testing of materials.

1. Introduction

In recent years much effort has been focussed on estimating the effective complex permittivity ϵ^* [2–4, 9, 10, 18, 19, 22, 23] of periodic and random media. In the present paper we formulate and solve the inverse problem: having measured the effective complex permittivity we want to make some conclusions about the volume fractions of the constituents and the geometry of the microstructure. We consider sea ice as an example of a random medium. Sea ice is a polycrystalline medium of pure ice with random brine and air inclusions on the millimetre scale. Its electromagnetic behaviour on this scale is quite complicated, and is governed by the complex permittivity $\epsilon(x)$, which varies spatially and admits very different values in the brine, ice and air. Many important features of sea ice such as age, type, salinity, temperature, thermal and fluid transport properties, growth history, etc, are related to the details of its microstructure. In particular, the geometry and relative volume fraction of the inclusions depend strongly on the temperature of the

0959-7174/98/040437+14$19.50

ice, the conditions under which the ice was grown, and the history of the sample under consideration.

In the quasistatic regime, when the wavelength λ is much larger than the microstructural scale, the wave cannot resolve variations in the local complex permittivity $\epsilon(x)$ on a fine scale, and the brine and air microstructure on the millimetre scale is averaged out, or 'homogenized'. The behaviour of the wave inside the sea ice in this case is primarily governed by its effective complex permittivity ϵ^*. For example, this is the case for synthetic aperture radar (SAR) used in remote sensing, which operates in the microwave region, such as in the C-band, with central frequency $f = 5.3$ GHz and free-space wavelength $\lambda = 5.7$ cm.

Various models and effective medium theories, such as the coherent potential approximation, have been used to derive 'mixing formulae' for ϵ^* of the system. Typically the sea ice was assumed to consist of a host medium, pure ice, containing ellipsoidal inclusions of brine and air (see [23, 25]). While mixing formulae are certainly useful, their applicability to the full range of microstructures is limited, and the assumptions under which they are derived are not always satisfied. A general analytic method for obtaining bounds on the bulk effective properties of composite materials was developed in [2, 3, 18, 19, 9], and applies to any two-component medium. This analytic method has been applied to sea ice in [10, 21, 11]. Given an increasing amount of information on the microstructure, such as the brine volume fraction, statistical isotropy, or the assumption that the brine phase is contained in separated inclusions (i.e. it does not form a connected matrix, or percolate), these bounds restrict all possible values of ϵ^* to increasingly smaller regions of the complex ϵ^* plane. However, as discussed before, it would be very useful to be able to deduce the detailed microstructural properties of the medium, such as the geometry and the volume fractions of the constituents, from electromagnetic measurements.

In the present paper, we invert the bounds on the effective complex permittivity to obtain 'inverse' bounds on structural parameters of a two-component mixture from given complex permittivity data. Two types of inverse bounds on the volume fractions of the constituents are derived: first-order bounds valid for general anisotropic two-component mixtures without any geometrical constraints, and second-order bounds for isotropic mixtures. We obtain both rigorous bounds on the possible range of volume fractions given a value of the observed complex permittivity, valid in the quasistatic regime, and an accurate algorithm for predicting the volume fraction associated with a given data set of permittivity values. The sea ice is a three-component mixture of brine, ice and air. To apply the developed algorithm, we modelled the three-component material as a mixture of brine and a composite formed by ice and air. This is a significant simplification of a problem for three-component materials which is possible due to the well known 'bubbly' structure of ice with a small volume fraction of air. The algorithm is demonstrated on a representative data set from [1], with excellent results.

It should be remarked that a similar idea of estimating structural parameters from homogenized measurements was used previously, and applied to multifrequency data for thin silver films [17]. Analytical expressions for first-order inverse bounds were derived in [6]. They were applied to the estimation of volume fraction of a polarizable component from multifrequency measurements of the effective complex conductivity of a geophysical mixture in [26]. Other approaches to the inversion for microstructural information have been considered in [8, 16, 14, 22]. The developed method is sufficiently general to be able to invert these bounds for much more detailed information about the microstructure, such as brine inclusion separation (which is intimately connected with temperature and percolation properties), but this is dealt with in [20].

2. Bounds for the effective complex permittivity

The bounds for the effective complex permittivity of a two-component mixture were obtained using the analytic continuation method [2, 3, 18, 9]. We consider a random medium in $\mathbb{R}^d$, where $d = 2$ or $d = 3$. Let $\epsilon(x, \eta)$ be a (spatially) stationary random field in $x \in \mathbb{R}^d$ and $\eta \in \Omega$, where Ω is the set of all realizations of the random medium. We assume $\epsilon(x, \eta)$ takes the values ϵ_1 in the brine and ϵ_2 in the ice, and write $\epsilon(x, \eta) = \epsilon_1\chi_1(x, \eta)+\epsilon_2\chi_2(x, \eta)$, where χ_j is the characteristic function of medium $j = 1, 2$, which equals one for all realizations $\eta \in \Omega$ having medium j at x, and equals zero otherwise. Let $E(x, \eta)$ and $D(x, \eta)$ be the stationary random electric and displacement fields, related by $D(x, \eta) = \epsilon(x, \eta)E(x, \eta)$, satisfying

$$\nabla \cdot D = 0 \qquad \nabla \times E = 0 \tag{1}$$

where $\langle E(x, \eta)\rangle = e_k$, e_k is a unit vector in the kth direction, for some $k = 1, \ldots, d$, and $\langle\cdot\rangle$ means ensemble average over Ω or spatial average over all of $\mathbb{R}^d$. The effective complex permittivity tensor $\boldsymbol{\epsilon}^*$ is defined as

$$\langle D\rangle = \boldsymbol{\epsilon}^*\langle E\rangle. \tag{2}$$

For simplicity, we focus on one diagonal coefficient $\epsilon^* = \epsilon^*_{kk}$. Due to homogeneity of effective parameters, $\epsilon^*(c\epsilon_1, c\epsilon_2) = c\epsilon^*(\epsilon_1, \epsilon_2)$ for any constant c, ϵ^* depends only on the ratio $h = \epsilon_1/\epsilon_2$, and we define $m(h) = \epsilon^*/\epsilon_2$. The two main properties of $m(h)$ are that it is analytic off $(-\infty, 0]$ in the h plane, and that it maps the upper half plane to the upper half plane [2, 9], so that it is an example of a Herglotz function. Based on this fact, a representation for ϵ^* was developed in [2] for periodic composites, and a general integral representation for ϵ^* was obtained in [9]. For $F(s) = 1 - m(h), s = 1/(1 - h)$, which is analytic off $[0, 1]$ in the s plane, the integral representation is

$$F(s) = 1 - \frac{\epsilon^*}{\epsilon_2} = \int_0^1 \frac{\mathrm{d}\mu(z)}{s - z} \qquad s = \frac{1}{1 - \epsilon_1/\epsilon_2} \tag{3}$$

where the positive measure μ on $[0, 1]$ is the spectral measure of the self-adjoint operator $\Gamma\chi_1$, where $\Gamma = \nabla(-\Delta)^{-1}\nabla\cdot$.

Statistical assumptions about the geometry are incorporated into μ through its moments μ_n. Comparison of a perturbation expansion of (3) around a homogeneous medium ($s = \infty$, or $\epsilon_1 = \epsilon_2$) with a similar expansion of a resolvent representation for $F(s)$ [9], yields

$$\mu_n = \int_0^1 z^n \,\mathrm{d}\mu(z) = (-1)^n\langle\chi_1[(\Gamma\chi_1)^n e_k]\cdot e_k\rangle. \tag{4}$$

Then $\mu_0 = p_1$ if the volume fractions p_1 and $p_2 = 1 - p_1$ of the brine and ice are known, and $\mu_1 = p_1p_2/d$ if the material is statistically isotropic. In general, knowledge of the $(n + 1)$-point correlation function of the medium allows calculation of μ_n (in principle).

Bounds on ϵ^*, or $F(s)$, are obtained by fixing s in (3), varying over admissible measures μ (or admissible geometries), such as those that satisfy only $\mu_0 = p_1$, and finding the corresponding range of values of $F(s)$ in the complex plane [4, 9, 18, 19]. Two types of bounds on ϵ^* are readily obtained. The first bound $D^{(1)}$ assumes only that the relative volume fractions p_1 and $p_2 = 1 - p_1$ are known, so that only $\mu_0 = p_1$ need be satisfied. In this case, the admissible set of measures forms a compact, convex set. Since (3) is a linear functional of μ, the extreme values of F are attained by extreme points of the set of admissible measures, which are the Dirac point measures of the form $p_1\delta_z$. The values of

F must lie inside the circle $p_1/(s-z)$, $-\infty \leqslant z \leqslant \infty$, and the region $D^{(1)}$ is bounded by circular arcs, one of which is parametrized in the F plane by

$$C_1(z) = \frac{p_1}{s-z} \qquad 0 \leqslant z \leqslant p_2. \tag{5}$$

To display the other arc, it is convenient to use the auxiliary function [2]

$$E(s) = 1 - \frac{\epsilon_1}{\epsilon^*} = \frac{(1-sF(s))}{s(1-F(s))} \tag{6}$$

which is a Herglotz function like $F(s)$, analytic off $[0, 1]$, with a representation like (3) whose representing measure has mass p_2. Then in the E plane, the other circular boundary of $D^{(1)}$ is parametrized by

$$\hat{C}_1(z) = \frac{p_2}{s-z} \qquad 0 \leqslant z \leqslant p_1. \tag{7}$$

In the ϵ^* plane (see figure 1), $D^{(1)}$ has vertices $A_1 = \epsilon_2(1 - C_1(0)) = p_1\epsilon_1 + p_2\epsilon_2$ and $B_1 = \epsilon_1/(1-\hat{C}_1(0)) = (p_1/\epsilon_1 + p_2/\epsilon_2)^{-1}$, and collapses to the interval $(p_1/\epsilon_1 + p_2/\epsilon_2)^{-1} \leqslant \epsilon^* \leqslant p_1\epsilon_1 + p_2\epsilon_2$ when ϵ_1 and ϵ_2 are real. In the last case, these bounds are the classical arithmetic (upper) and harmonic (lower) mean bounds. The complex bounds (5) and (7) are optimal and can be attained by a composite of uniformly aligned spheroids of material 1 in all sizes coated with confocal shells of material 2 and vice versa [18, 19]. These arcs are traced out as the aspect ratio varies. When the volume fractions of the components in the mixture vary, the corresponding domains $D^{(1)}$ cover the region $D_0^{(1)}$, a general bound on ϵ^* for arbitrary composites mixed from the initial materials.

If the mixture is further assumed to be statistically isotropic, i.e. $\epsilon^*_{ik} = \epsilon^*\delta_{ik}$, then $\mu_1 = p_1p_2/d$ must be satisfied as well. A convenient way of including this information is to use the transformation introduced in [4]:

$$F_1(s) = \frac{1}{p_1} - \frac{1}{s\,F(s)}. \tag{8}$$

The function $F_1(s)$ is, again, a Herglotz function having a representation like (3) with representing measure μ^1, with only a restriction on its mass $\mu_0^1 = p_2/p_1d$.

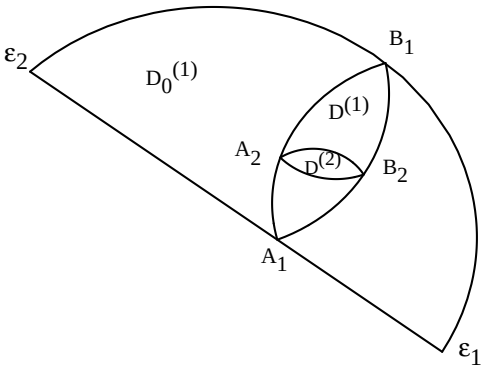

Figure 1. Illustration of bounds on the bulk permittivity of a two-component mixture. For a given volume fraction of one component, all possible effective permittivities of the mixture lie in the lens shaped region $D^{(1)}$, whereas isotropic mixtures lie in the smaller lens shaped domain $D^{(2)}$. All possible bulk permittivities of mixtures with arbitrary volume fractions lie in the region $D_0^{(1)}$ which is a union of the domains $D^{(1)}$ over all volume fractions.

Applying the same procedure as for $D^{(1)}$ yields a region $D^{(2)}$, whose boundaries are again circular arcs. In the F plane, one of these arcs is parametrized by

$$C_2(z) = \frac{p_1(s-z)}{s(s-z-p_2/d)} \qquad 0 \leqslant z \leqslant (d-1)/d. \tag{9}$$

In the E plane, the other arc is parametrized by

$$\hat{C}_2(z) = \frac{p_2(s-z)}{s(s-z-p_1(d-1)/d)} \qquad 0 \leqslant z \leqslant 1/d. \tag{10}$$

In the ϵ^* plane, $D^{(2)}$ has vertices A_2 and B_2 (see figure 1), and collapses to the interval

$$\epsilon_2 + p_1\left(\frac{1}{\epsilon_1-\epsilon_2}+\frac{p_2}{d\epsilon_2}\right)^{-1} \leqslant \epsilon^* \leqslant \epsilon_1 + p_2\left(\frac{1}{\epsilon_2-\epsilon_1}+\frac{p_1}{d\epsilon_1}\right)^{-1} \tag{11}$$

when ϵ_1 and ϵ_2 are real with $\epsilon_1 \geqslant \epsilon_2$. These are the Hashin–Shtrikman bounds [13]. When $\epsilon_1 \leqslant \epsilon_2$, the sequence of inequalities is reversed. The vertices A_2 and B_2 (which correspond to the expressions in (11)), are attained by the Hashin–Shtrikman coated sphere geometries (spheres of all sizes of material of permittivity ϵ_1 in the volume fraction p_1 coated with spherical shells of material ϵ_2 in the volume fraction p_2 and vice versa), and lie on the arcs which bound $D^{(1)}$.

3. Inverse bounds for structural parameters

From equations (3) it immediately follows that the effective complex permittivity of the mixture of two constituents can be represented as an integral with some positive Borel measure $\mu\,(\mathrm{d}z)$ on unit interval:

$$\epsilon^* = \epsilon_2 - \epsilon_2\ F_\mu(s) = \epsilon_2 - \epsilon_2 \int_0^1 \frac{\mu\,(\mathrm{d}z)}{s-z} \tag{12}$$

where $F_\mu = 1-\epsilon^*/\epsilon_2$ and $s = 1/(1-\epsilon_1/\epsilon_2),\ s \notin [0,1]$. An important feature of the integral representation (12) of the effective property is that it separates the properties of the mixture constituents, which are contained in the variable s, from the structural information about the geometry of the mixture, which is contained in the measure μ. Wishing to recover this geometrical information from the measurements of the effective complex permittivity, we need to describe a set of measures μ which generates a measured value ϵ^* for the effective property:

$$\mathcal{M}(\mu) = \{\mu : F_\mu(s) = 1-\epsilon^*/\epsilon_2\}. \tag{13}$$

The structural information about the geometry of the mixture is contained in the moments μ_n of the measure μ (see equation (4)). Using an expansion of $F(s)$ for $|s| > 1$ about a homogeneous medium

$$F(s) = \frac{\mu_0}{s} + \frac{\mu_1}{s^2} + \cdots \qquad \mu_n = \int_0^1 z^n\ \mathrm{d}\mu(z) \tag{14}$$

the moments of the measure μ can be determined. If all the moments are known, then the measure μ is uniquely determined. Theoretically, if only a measured value of the effective permittivity is given, we cannot determine the moments, nor the structure of the material. This is because there can exist a great variety of structures generating the same response under the applied field. But instead, we can determine an interval confining the first moment of the measure μ. This will give us an interval of uncertainty for the volume fraction of

one material in a mixture for a general anisotropic medium with no assumptions on the geometrical structure.

To obtain information about other structural parameters, we can parametrize a subset M of $\mathcal{M}$ in (13) which consists of singular measures $\tilde{\mu}$ concentrated on points τ from the interval $[0, 1]$. Geometrically, this corresponds to the parametrization of the set of possible microstructures using 'coated sphere' composites: inclusions of one material coated with the second material. For the measures from this subset M the corresponding value of F is given by

$$F(s) = \frac{\alpha}{s - \tau}. \tag{15}$$

For the zeroth-order bounds on the complex permittivity given by the domain $D_0^{(1)}$ in figure 1, $0 \leqslant \alpha \leqslant 1$, $0 \leqslant \tau \leqslant 1$ and $F(1) \leqslant 1$, which produces all possible ϵ^* formed from the initial materials. Now, having a prescribed value for $F(s)$ we want to find the appropriate intervals for α and τ.

The interval for α gives us an interval of uncertainty for the volume fraction p_1 of one material in the mixture,

$$p_{\mathrm{l}}^{(1)} \leqslant p_1 \leqslant p_{\mathrm{u}}^{(1)} \tag{16}$$

while the corresponding values for τ estimate the support of possible Dirac measures $\tilde{\mu}$ from the set M which are equivalent to the true spectral measure from the point of view of the measured value of ϵ^*:

$$\tilde{\mu}_{\mathrm{l}}^{(1)} = p_{\mathrm{l}}^{(1)}\,\delta(z_{\mathrm{l}}^{(1)}) \qquad \tilde{\mu}_{\mathrm{u}}^{(1)} = p_{\mathrm{u}}^{(1)}\,\delta(z_{\mathrm{u}}^{(1)}) \qquad \tilde{\mu} \in M. \tag{17}$$

The measures $\tilde{\mu}_{\mathrm{l}}^{(1)}$ and $\tilde{\mu}_{\mathrm{u}}^{(1)}$ are on the boundary of the set $\mathcal{M}$.

By changing τ in (15) the corresponding structures trace out the arcs (A_1, A_2, B_1) or (A_1, B_2, B_1) (see figure 1) changing from the laminates (in 2D case) or cylinders (in 3D case) oriented along the field through coated spheroids with varying aspect ratio to isotropic structures and then to laminates (or cylinders) oriented across the field. Hence the last estimate for the measure support can be extended into an estimate for geometrical parameters such as, for example, the degree of an anisotropy of the mixture [20].

These are the first-order bounds. However, if some information about the structure of the composite is available, then bounds can be derived for the next moments, and the uncertainty intervals will be essentially decreased. Pursuing this approach for isotropic materials, we use the second-order expansion for the function F. Therefore the inverse bounds for the volume fraction of a component in an isotropic mixture can be referred to as second-order inverse bounds.

Exploiting the transformation (8) from the function F to the function F_1 preserves the type of integral representation

$$F_1(s) = \int_0^1 \frac{\mu^1(\mathrm{d}z)}{s - z}. \tag{18}$$

Hence the same approach works here as well. We can also determine the support of equivalent measures $\tilde{\mu} \in M$

$$\tilde{\mu}_{\mathrm{l}}^{(2)} = p_{\mathrm{l}}^{(2)}\,\delta(z_{\mathrm{l}}^{(2)}) \qquad \tilde{\mu}_{\mathrm{u}}^{(2)} = p_{\mathrm{u}}^{(2)}\,\delta(z_{\mathrm{u}}^{(2)}) \qquad \tilde{\mu} \in M \tag{19}$$

and an admissible interval for the second moment of the measure, which gives us an interval of uncertainty for the volume fraction for an isotropic medium, or the second-order bounds:

$$p_{\mathrm{l}}^{(2)} \leqslant p_1 \leqslant p_{\mathrm{u}}^{(2)}. \tag{20}$$

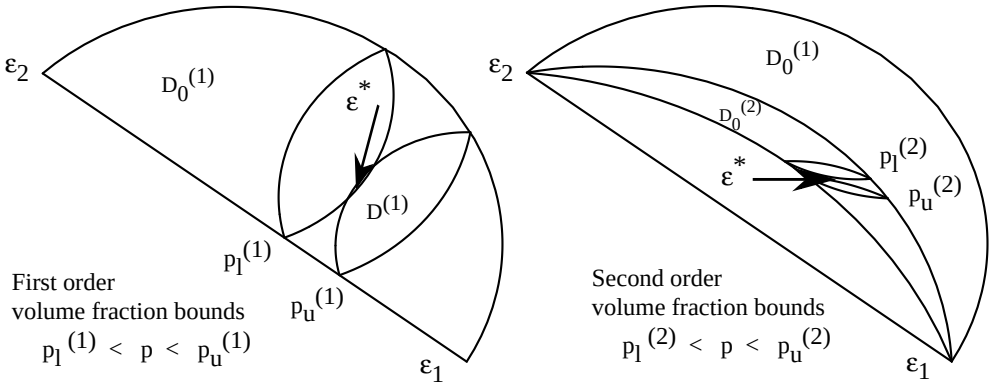

Figure 2. Illustration of bounds on the volume fraction of one component in the mixture derived from the first-order anisotropic bounds (left-hand diagram) and from the second-order isotropic bounds (right-hand diagram) for the effective permittivity. The small lens shaped domains each contain the anisotropic (left) and isotropic (right) mixtures corresponding to the volume fractions of the first component $p_{\rm l}$ and $p_{\rm u}$. These points give the lower and upper estimates for the volume fraction of the first material in the mixture.

A geometrical illustration of the idea of the inversion is shown in figure 2.

Given an observed complex permittivity value ϵ^*, we increase the volume fraction p_1 in the bound $D^{(1)}$ until one of the circular arcs on the boundary of $D^{(1)}$ touches the point ϵ^*. This defines the lower bound $p_{\rm l}^{(1)}$ on the possible range of volume fractions associated with the data point. Similarly, we decrease p_1 until the other arc touches the data point, giving an upper bound $p_{\rm u}^{(1)}$ on the possible range of the volume fractions. Applying the same procedure to the isotropic complex bound $D^{(2)}$ yields even tighter lower $p_{\rm l}^{(2)}$ and upper $p_{\rm u}^{(2)}$ bounds on the volume fraction p_1.

Given a set of data points $\epsilon^*(k)$ for a set of N measurements, $k = 1, \ldots, N$, we carry out the inversion for each point, and then take the maximum over k of the $p_{\rm l}^{(1)}$ and the minimum over k of the $p_{\rm u}^{(1)}$, and similarly for $p_{\rm l}^{(2)}$ and $p_{\rm u}^{(2)}$, which yield rather tight, accurate estimates of the volume fractions in the mixture associated with the given data set.

Using this unified approach we rederive below the first-order bounds on the volume fraction of a component in an anisotropic mixture, derived in [6], in the complex ϵ^* plane. Then assuming isotropy of the mixture, we derive the bounds for the volume fraction in an isotropic mixture. These are the second-order bounds. We then apply the technique developed here to real measurements of the complex permittivity of sea ice and compare our bounds with experimental results.

4. First- and second-order inverse bounds

Let f be the value of F corresponding to the measured effective complex permittivity ϵ^* for the given properties ϵ_1, ϵ_2 of the constituents. As shown above, if we do not input any geometrical information about the mixture, aside from the volume fractions, the value of f lies inside the circular arc

$$C_1(z) = \frac{p_1}{s - z} \qquad 0 \leqslant z \leqslant p_2. \tag{21}$$

We vary p_1 so that the given value f lies on this arc and we obtain an equation for the lower bound on the structural parameters $\{p_1, z\}$:

$$p_1 = f\,(s - z). \tag{22}$$

Solving it, we find the lower first-order bounds $p_1^{(1)}$ and $z_1^{(1)}$ for the volume fraction p_1 and the support of the measure $\mathrm{supp}(\tilde{\mu})$:

$$z_1^{(1)} = \frac{\mathrm{Im}\,(fs)}{\mathrm{Im}\,(f)} \qquad p_1^{(1)} = |f|^2\,\frac{\mathrm{Im}\,(\bar{s})}{\mathrm{Im}\,(f)}. \tag{23}$$

Here the bar in the second expression denotes the complex conjugate. The value of $z_1^{(1)}$ in (23) gives the bound for the interval of variation of the support of the measure $\tilde{\mu}$ in (15), $p_1^{(1)}$ gives the lower bound for the first moment of the measure $\tilde{\mu}$ or its mass in (15). But the first moment of the measure $\tilde{\mu}$ equals the first moment of the true measure μ: $\tilde{\mu}_0 = \mu_0$. Hence $p_1^{(1)}$ gives a rigorous bound for the volume fraction of the first component in the mixture.

In order to obtain the other bound, we can consider an auxiliary function $G(t)$ [4]:

$$G(t) = \frac{\epsilon_1 - \epsilon^*}{\epsilon_1} = \frac{1 - s\,F(s)}{1 - s} \tag{24}$$

with the same properties as F for some positive measure ν. The advantage to using this function as opposed to $E(s)$ is that the spectrum (or support of μ in (3)) is trivially transformed via $t = 1 - s$, so that spectral bounds obtained for F are easily translated over to G, which is not the case for E. The value g of the function G corresponding to the measured ϵ^*, lies on the arc

$$\tilde{C}_1(z) = \frac{p_2}{t - z} \qquad 0 \leqslant z \leqslant p_1 \tag{25}$$

hence we can derive bounds for z and $p_2 = 1 - p_1$ similar to those considered above. The formulae are analogous to (23), switching p_1 for p_2, f for g, and s for $t = 1 - s$. Thus we obtain the upper bound p_u for the volume fraction of the first component and the corresponding bound for the supporting z_u:

$$z_\mathrm{u} = \frac{\mathrm{Im}\,(g\,t)}{\mathrm{Im}\,(g)} \qquad p_\mathrm{u} = \frac{\mathrm{Im}\,(g\,\bar{g}\,\bar{t})}{\mathrm{Im}\,(g)}. \tag{26}$$

The estimate for the support of the measure $\tilde{\mu}$ is obtained as $z_\mathrm{u}^{(1)} = 1 - z_\mathrm{u}$, because from the auxiliary relationship

$$F(1 - t) = \frac{1 - t\,G(t)}{1 - t} \tag{27}$$

it follows that poles of the functions F and G sum up to unity. Simplifying (26), we obtain the first-order bounds for the measure support and the volume fraction:

$$z_\mathrm{u}^{(1)} = 1 - \frac{\mathrm{Im}\,(g\,t)}{\mathrm{Im}\,(g)} \qquad p_\mathrm{u}^{(1)} = 1 - \frac{|g|^2\,\mathrm{Im}\,(\bar{t})}{\mathrm{Im}\,(g)}. \tag{28}$$

Now, assume that the mixture under consideration is known to be isotropic, which means that the measured ϵ^* has to belong to the domain $D^{(2)}$ (see figure 1). In order to derive second-order bounds on the volume fraction of one component in a two-component isotropic mixture, we consider the boundary $C_2(z)$ in (9) of the circle containing the point f inside:

$$F(s) = \frac{p_1(s - z)}{s(s - z - p_2/d)} \qquad 0 \leqslant z \leqslant (d - 1)/d \tag{29}$$

and choose the parameters such that the value f lies on the admissible part of the arc $C_2(z)$. Separating real and imaginary parts we obtain a system of equations for z and p_1. Solving the system we need to choose a solution of (29) which satisfies $0 \leqslant z \leqslant (d-1)/d$:

$$\{p_1,\ z\}: \quad 0 \leqslant z \leqslant (d-1)/d. \tag{30}$$

In order to obtain the other bound we again consider the auxiliary function $G(t)$ (24), which is obtained from the function $F(s)$ by changing p_1 for $p_2 = 1 - p_1$ and s for $t = 1 - s$. The explicit formulae are as follows. Let us introduce complex parameters v and w as

$$v = \frac{\epsilon_1\,(\epsilon^* - \epsilon_2)}{\epsilon^*\,(\epsilon_1 - \epsilon_2)} = \frac{t(1-w)}{t-w} \qquad w = \frac{\epsilon_1 - \epsilon^*}{\epsilon_1 - \epsilon_2} = \frac{t(1-v)}{t-v}. \tag{31}$$

The second-order bounds $\{p_{\mathrm{l}}^{(2)}, z_{\mathrm{l}}^{(2)}\}$, and $\{p_{\mathrm{u}}^{(2)}, z_{\mathrm{u}}^{(2)}\}$, for the structural parameters are given by the pair of solutions of (29) and the similar problem for the transformed function G:

$$\begin{aligned} p_{\mathrm{l}}^{(2)} &= Q(v,s) \qquad & z_{\mathrm{l}}^{(2)} &= R(v,s) \\ p_{\mathrm{u}}^{(2)} &= 1 - Q(w,s) \qquad & z_{\mathrm{u}}^{(2)} &= 1 - R(w,s) \end{aligned} \tag{32}$$

such that the constraint (30) (and the corresponding auxiliary constraint) is satisfied. Here Q and R are

$$\begin{aligned} Q(v,s) &= \frac{2dv_{\mathrm{r}}s_{\mathrm{i}} + v_{\mathrm{i}} - \sqrt{T}}{2(ds_{\mathrm{i}} + v_{\mathrm{i}})} \\ R(v,s) &= \frac{2dv_{\mathrm{i}}(1-s_{\mathrm{r}}) - v_{\mathrm{i}} - \sqrt{T}}{2dv_{\mathrm{i}}} \\ T &= v_{\mathrm{i}}(v_{\mathrm{i}} - 4ds_{\mathrm{i}}|v|^2 + 4dv_{\mathrm{r}}s_{\mathrm{i}} - 4d^2v_{\mathrm{i}}s_{\mathrm{i}}^2) \end{aligned} \tag{33}$$

and the subscripts refer to the real or imaginary parts.

It is shown in [5] that the support of the measure μ is directly related to the separation distance between the particles in matrix–particle composite. Based on the approach developed here, we extract structural information about separation between the brine inclusions in [20].

The geometrical idea of the second-order bounds in the complex ϵ^* plane is illustrated in figure 2. Complex permittivities of all possible mixtures formed from two materials with the complex permittivities ϵ_1 and ϵ_2 and arbitrary volume fraction of the constituents are confined to the region $D_0^{(1)}$. The composites with isotropic structure and arbitrary volume fraction belong to the smaller region $D_0^{(2)}$, which is a union of small lens shaped domains corresponding to isotropic mixtures for all volume fractions. Two such domains are shown in figure 2 for the volume fractions of the first material equal to 0.5 and 0.56. Inverse bounds for the volume fraction $[p_{\mathrm{l}}^{(2)},\ p_{\mathrm{u}}^{(2)}]$ provide a range of variation of the volume fraction parameter $p = p_1$ for all such small domains which could possibly contain the measured value of ϵ^*.

For measurements corresponding to different frequencies, the inverse bounds for the volume fraction of a component were derived in [17, 6, 26] as an intersection of particular bounding intervals. In determination of the brine volume fraction in sea ice below, we consider the case where several measurements are made at the same temperature and the same physical conditions. In this situation, we believe that, though we deal with slightly different microstructures, we do not have means to distinguish them. Hence as well as for frequency dependent measurements, it is the same structure, and the bounds for the volume fraction are an intersection of all particular bounds, corresponding to particular measurements.

For a set of data points corresponding to the same structure the bounds are given by an intersection of all admissible intervals. Suppose we have several measurements $\epsilon^*(k)$, $k = 1, \ldots, N$, corresponding to the same composite structure which means that we do not distinguish differences in geometry of the mixtures. We find that the intersection over k of the intervals $p_{\rm l}^{(q)}(k) \leqslant p \leqslant p_{\rm u}^{(q)}(k)$ gives the bounds for the volume fraction $p = p_1$:

$$P_{\rm l}^{(q)} = \max_k \, p_{\rm l}^{(q)}(k) \leqslant p \leqslant \min_k \, p_{\rm u}^{(q)}(k) = P_{\rm u}^{(q)} \qquad q = 1, 2. \tag{34}$$

Here $p_{\rm l}^{(q)}(k)$ and $p_{\rm u}^{(q)}(k)$ are, respectively, lower and upper bounds for the volume fraction derived from the effective complex permittivity $\epsilon^*(k)$ and q is the order of the bounds, $q = 1$ for a general mixture, $q = 2$ for an isotropic mixture.

5. Inverse bounds for the sea-ice brine volume from measured effective complex permittivities

Determination of the structure of sea ice and brine content from measurements of the effective complex permittivity is an important problem in remote sensing. We apply the developed method to two data sets of 4.75 GHz measurements of the effective complex permittivity of sea ice [1]. The data sets each contain nine measurements of the effective complex permittivity of sea ice for two different temperatures and for different volume fractions of brine. The temperatures are -6 °C and -11 °C. Given a sea-ice sample of temperature T °C and salinity S parts per thousand (ppt), the brine volume p_1 is calculated from the equation of Frankenstein and Garner [7]. Given the frequency f GHz as well, the complex permittivity ϵ_2 of the brine is computed from the equations of Stogryn and Desargant [24]. Furthermore, although the brine microstructure tends to be elongated in the vertical direction, since only vertically incident waves are considered in [1], we are justified in assuming that the geometry is isotropic within the horizontal plane, in which case we take $d = 2$ above. These parameter calculations gave generally good agreement with the bounds $D^{(1)}$ and $D^{(2)}$ in [10]. However, we found that closer agreement is obtained if we slightly adjust the complex permittivity ϵ_2 of the ice by treating it as a composite with a small volume fraction of air, and calculating its effective permittivity ϵ_2 with the Maxwell–Garnett formula [15].

Sea ice is a mixture of three components: pure ice, brine and air with the unit complex permittivity of air, $\epsilon_{\rm air} = 1$, the complex permittivity of ice $\epsilon_{\rm ice} = 3.15 + {\rm i}\,0.002$, and the complex permittivity of brine depending on the temperature and frequency. We consider this three-component mixture as obtained in a two-step mixing procedure: a composite of ice and air is mixed with brine. We assume that the first mixture of ice and air is a 3D isotropic composite of an ice matrix containing inclusions of air. As the volume fraction of the air inclusions is small, and the permittivities of ice and air are relatively close, a good approximation of the effective complex permittivity of such a mixture is given by the Maxwell–Garnett formula for a two-phase composite

$$\epsilon_2 = \epsilon_{\rm ice}\left[1 - \frac{d\; p_{\rm air}(\epsilon_{\rm ice} - \epsilon_{\rm air})}{\epsilon_{\rm ice}(d-1) + \epsilon_{\rm air} + p_{\rm air}(\epsilon_{\rm ice} - \epsilon_{\rm air})}\right]. \tag{35}$$

The Maxwell–Garnett formula, as well as Bruggeman's symmetric effective medium formula [15], gives close results for the effective complex permittivity of the mixture of ice and air. When the volume fraction of air in this mixture changes, the regions $D_0^{(1)}$, $D^{(1)}$ and $D^{(2)}$ confining the possible effective permittivities of sea ice, change their location in the

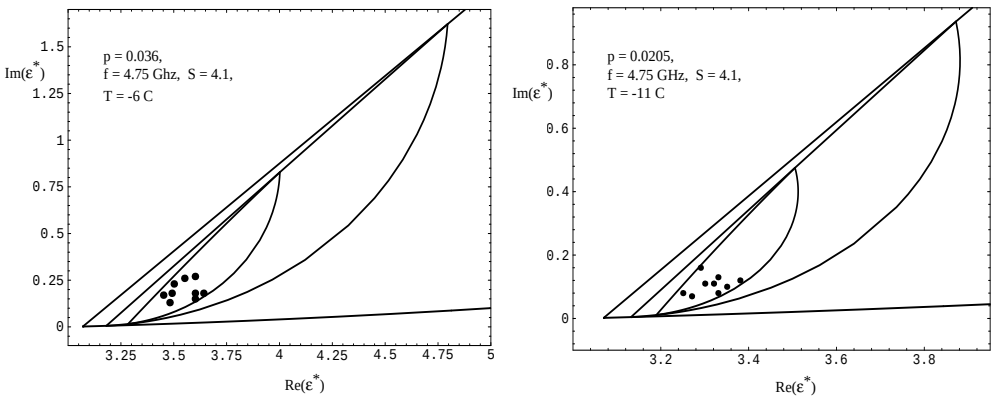

Figure 3. Experimentally measured complex permittivity values for sea-ice samples with brine volume $p = 0.036$ (data set 1, left-hand diagram) and with brine volume $p = 0.0205$ (data set 2, right-hand diagram), and bounds for the complex permittivity of composites formed from the brine and ice/air mixture with the corresponding volume fractions. The bigger lens shaped region $D^{(1)}$ corresponds to all anisotropic composites, and the smaller lens shaped region $D^{(2)}$ confines the complex permittivities of two-dimensional isotropic mixtures. Points show the measured values of the complex permittivity of sea ice containing the given percentage of brine.

complex ϵ^* plane (see figures 1 and 2). The air volume fraction in the ice/air mixture was chosen so that the region $D^{(2)}$ corresponding to 2D isotropic composites would contain all points of measurements from both data sets. This gives 2.5% of air in the ice/air mixture and the value for permittivity $\epsilon_2 = 3.07 + \mathrm{i}\,0.0019$. We used this value as the complex permittivity of the ice/air component in an ice/air/brine mixture. The complex permittivity of the other component, brine, depends on the temperature, and it is $\epsilon_2 = 51 + \mathrm{i}\,45$ for the first set of measurements at the temperature $-6\ ^\circ$C, and $\epsilon_2 = 42.2 + \mathrm{i}\,45.6$ for the second set of data at the temperature -11°C. These data sets are shown in figure 3. (We remark that the volume fraction of air could also be calculated *a priori* from knowledge of the density as in [11]).

First-order inverse bounds. For each particular data point from data sets 1 and 2, we used our technique to evaluate the brine volume from the measurements of the effective complex permittivity. As a first step we applied the bounds (23) and (28) for a general medium without any geometrical information.

For data set 1 with the volume fraction of brine $p = 0.036$, the intersection of all particular admissible intervals for the brine volume fraction gives an estimate as $0.0213 \leqslant p \leqslant 0.0664$. For data set 2 with the volume fraction of brine $p = 0.0205$, this estimate is $0.0119 \leqslant p \leqslant 0.0320$.

Second-order inverse bounds. The second-order inverse bounds for the brine volume fraction were derived from the measurements of the effective complex permittivity with the assumption of 2D isotropy of the mixture. The intersection of the bounding intervals for data set 1 with brine volume $p = 0.036$, estimates the brine volume as $0.0333 \leqslant p \leqslant 0.0422$. For data set 2 with volume fraction of brine $p = 0.0205$, the inverse bounds for the brine volume are $0.0189 \leqslant p \leqslant 0.0213$. The algorithm estimates the brine volume well within 10% error of the actual value of 0.0205 for data set 2.

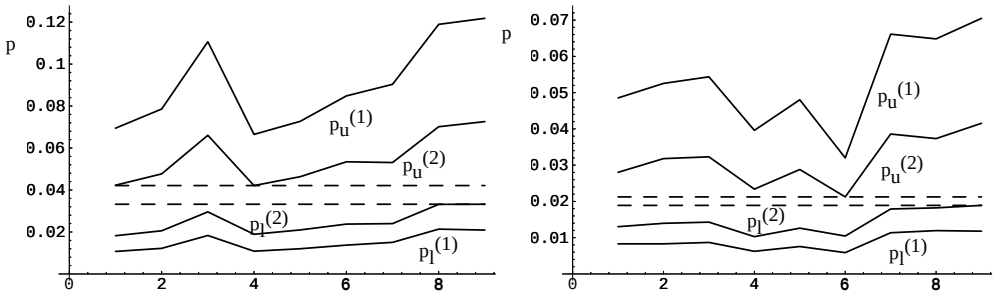

Figure 4. Comparison of the first- and second-order bounds for data set 1 with the actual brine volume of 0.036 (left-hand diagram) and data set 2 with the actual brine volume of 0.0205 (right-hand diagram). Joint plots of $p_{\mathrm{l}}^{(1)}(k)$ and $p_{\mathrm{u}}^{(1)}(k)$ show the first-order inverse bounds for general anisotropic composites, while plots of $p_{\mathrm{l}}^{(2)}(k)$ and $p_{\mathrm{u}}^{(2)}(k)$ show second-order inverse bounds for isotropic mixtures, where k denotes the index of the data point $k = 1, 2, \ldots, 9$. The dashed lines show the interval of uncertainty in determining the brine volume derived with the assumption of 2D isotropy.

Comparison of the first- and second-order bounds for each particular data point is shown in figure 4 for data sets 1 and 2. On the horizontal axis is shown the index of the data point. The points of the lower bound p_{l} and of the upper bound p_{u} corresponding to all nine different data points are joined on the plots to give better exposition. The shape of the curves is not important, because the numeration of the data points in the data sets is arbitrary, but the distance between the lower and upper curves is important.

In figure 4 the points corresponding to the first-order inverse bounds $p_{\mathrm{l}}^{(1)}(k)$ and $p_{\mathrm{u}}^{(1)}(k)$ are plotted, giving the lower and upper estimates. The maximum of $p_{\mathrm{l}}^{(1)}(k)$ and the minimum of $p_{\mathrm{u}}^{(1)}(k)$ with respect to k give the first-order inverse bounds for general anisotropic composites. For both data sets these are not very tight, permitting quite a large range of variation for the volume fraction. The second-order bounds $p_{\mathrm{l}}^{(2)}$ and $p_{\mathrm{u}}^{(2)}$ derived with the assumption about 2D isotropy of the composite, are shown for the same data sets. Again the points of the lower bound $p_{\mathrm{l}}^{(2)}(k)$ and of the upper bound $p_{\mathrm{u}}^{(2)}(k)$ for nine different data points, $k = 1, \ldots, 9$, are joined on the plot. In this case the interval of uncertainty is reduced by more than half compared with the first-order estimate.

The geometrical structure of the composites in each of the two sets of measurements is believed to vary negligibly, reflecting the similarity of the physical conditions of the experiments. Therefore the bounds for the volume fraction have to satisfy all particular restrictions, and are given by the intersection of all particular volume fraction intervals.

6. Conclusion

We have developed a unified approach to the problem of inverse bounds on the microstructural parameters of a mixture. Two types of inverse bounds are derived using the analyticity of the effective complex permittivity of the composite. They are first-order inverse bounds on the volume fraction and structural parameters for general anisotropic mixtures, and second-order inverse bounds for mixtures with 2D or 3D isotropic geometrical structure. The inclusion of additional information on geometrical structure of the composite considerably improves the inverse structural bounds. This is an expected result, because introducing isotropic restrictions for a geometrical structure, we restrict the class of the

composites. The inverse bounds obtained are used to estimate sea-ice brine volume from real measurements of the effective complex permittivity of sea ice. The bounds are in very good agreement with the experimental results.

Acknowledgments

We would like to thank Christopher Orum for very helpful comments on the manuscript. This work was supported by ONR grant N0000149310141 and NSF grants DMS-9622367 and OPP-9725038.

References

[1] Arcone S A, Gow A J and McGrew S 1986 Structure and dielectric properties at 4.8 and 9.5 GHz of saline ice *J. Geophys. Res.* **91** (C12) 14 281–303
[2] Bergman D J 1978 The dielectric constant of a composite material—a problem in classical physics *Phys. Rep.* C **43** 377–407
[3] Bergman D J 1980 Exactly solvable microscopic geometries and rigorous bounds for the complex dielectric constant of a two-component composite material *Phys. Rev. Lett.* **44** 1285
[4] Bergman D J 1982 Rigorous bounds for the dielectric constant of a two-component composite *Ann. Phys.* **138** 78
[5] Bruno O 1991 The effective conductivity of strongly heterogeneous composites *Proc. R. Soc.* A **433** 353–81
[6] Cherkaeva E and Tripp A C 1996 Bounds on porosity for dielectric logging *Proc. 9th Conf. of the European Consortium for Mathematics in Industry (ECMI96, Denmark, 1996)* (Lyngby: Technical University of Denmark) pp 304–6
[7] Frankenstein G and Garner R 1967 Equations for determining the brine volume of sea ice from -0.5° to -22.9° C *J. Glaciology* **6** (48) 943–4
[8] Gajdardziska-Josifovska M, McPhedran R C, McKenzie D R and Collins R E 1989 Silver–magnesium fluoride cermet films. 2: optical and electrical properties *Appl. Opt.* **28** 2744–53
[9] Golden K and Papanicolaou G 1983 Bounds on effective parameters of heterogeneous media by analytic continuation *Commun. Math. Phys.* **90** 473–91
[10] Golden K 1995 Bounds on the complex permittivity of sea ice *J. Geophys. Res. (Oceans)* **100** (C7) 699–711
[11] Golden K M 1997 The interaction of microwaves with sea ice *Wave Propagation in Complex Media (IMA Volumes in Mathematics and its Applications 96)* ed G Papanicolaou (Berlin: Springer) pp 75–94
[12] Hallikainen M 1992 Microwave remote sensing of low-salinity sea ice *Microwave Remote Sensing of Sea Ice (Geophysical Monograph 68)* ed F D Carsey (AGU) pp 361–73
[13] Hashin Z and Shtrikman S 1962 A variational approach to the theory of the effective magnetic permeability of multiphase materials *J. Appl. Phys.* **33** 3125–31
[14] Haslund E and Nost B 1998 Determination of porosity and formation factor of water-saturated porous specimens from dielectric dispersion measurements *Geophysics* **63** 149–53
[15] Landauer R 1978 Electrical conductivity in inhomogeneous media *Electrical, Transport and Optical Properties of Inhomogeneous Media (ETOPIM, Ohio State University, Columbus, OH, 1977)* (New York: American Institute of Physics)
[16] McPhedran R C, McKenzie D R and Milton G W 1982 Extraction of structural information from measured transport properties of composites *Appl. Phys.* A **29** 19–27
[17] McPhedran R C and Milton G W 1990 Inverse transport problems for composite media *Mat. Res. Soc. Symp. Proc.* **195** 257–74
[18] Milton G W 1980 Bounds on the complex dielectric constant of a composite material *Appl. Phys. Lett.* **37** 300–2
[19] Milton G W 1981 Bounds on the complex permittivity of a two component composite material *J. Appl. Phys.* **52** 5286–93
[20] Orum C, Cherkaeva E and Golden K M 1998 Recovery of inclusion separations in a composite from effective property measurements, in preparation
[21] Sawicz R and Golden K 1995 Bounds on the complex permittivity of matrix–particle composites *J. Appl. Phys.* **78** 7240–6

[22] Sen P N 1981 Relation of certain geometrical features to the dielectric anomaly of rocks *Geophysics* **46** 1714–20
[23] Sihvola A H and Kong J A 1988 Effective permittivity of dielectric mixtures *IEEE Trans. Geosci. Remote Sensing* **26** 420–9
[24] Stogryn A and Desargant G J 1985 The dielectric properties of brine in sea ice at microwave frequencies *IEEE Trans. Antenn. Propagat.* **AP-33** 523–32
[25] Tinga W R, Voss W A G and Blossey D F 1973 Generalized approach to multiphase dielectric mixture theory *J. Appl. Phys.* **44** 3897–902
[26] Tripp A C, Cherkaeva E and Hulen J 1998 Bounds on the complex conductivity of geophysical mixtures *Geophys. Prospecting* **46** in press